Am J Nucl Med Mol Imaging 2025;15(2):55-64
www.ajnmmi.us /ISSN:2160-8407/ajnmmi0162797

Original Article

Automatic synthesis of a phosphodiesterase 4B (PDE4B) radioligand and PET imaging in depression rodent models

Chenchen Dong[1*], Weijian Ye[1*], Yi Xu[2], Jiahui Chen[3], Kai Liao[1], Huiyi Wei[1], Yuanfang Jiang[1], Lu Hou[1], Junjie Wei[1], Zhiqiang Tan[1], Zhendong Song[3], Yinlong Li[3], Achi Haider[3], Hongjie Yuan[4], Steven H Liang[3], Lu Wang[1,5]

[1]Center of Cyclotron and PET Radiopharmaceuticals, Department of Nuclear Medicine and Key Laboratory of Basic and Translational Research on Radiopharmaceuticals, The First Affiliated Hospital of Jinan University, Guangzhou 510630, Guangdong, China; [2]Department of Cardiology, The First Affiliated Hospital of Jinan University, Guangzhou 510630, Guangdong, China; [3]Department of Radiology and Imaging Sciences, Emory University, 1364 Clifton Road, Atlanta, GA 30322, USA; [4]Department of Pharmacology and Chemical Biology, Emory University, 1364 Clifton Road, Atlanta, GA 30322, USA; [5]The Guangzhou Key Laboratory of Basic and Translational Research on Chronic Diseases, Jinan University and Department of Pharmacy, The First Affiliated Hospital of Jinan University, Guangzhou 510630, Guangdong, China. [*]Equal contributors.

Received December 19, 2024; Accepted March 23, 2025; Epub April 15, 2025; Published April 30, 2025

Abstract: Phosphodiesterase 4B (PDE4B) is an enzyme that hydrolyzes cyclic adenosine monophosphate (cAMP), a critical signaling molecule involved in various cellular processes. Dysregulated PDE4B activity has been implicated in psychiatric diseases like depression and schizophrenia. In this report, a PDE4B-targeted PET tracer, [^{18}F]PF-06445974, was synthesized using an automated synthesis module. [^{18}F]PF-06445974 demonstrated high brain specificity, robust uptake, and excellent stability. *In vivo* metabolic studies confirmed that its radioactive metabolites did not cross the blood-brain barrier, and no abnormal bone uptake was observed in PET imaging. Furthermore, PET studies and quantitative autoradiography revealed significantly increased expression of PDE4B in the hippocampus and cortex of depression model rats compared to normal controls. The findings highlight the potential of *in vivo* PDE4B PET imaging as a valuable tool for monitoring PDE4B changes in depression, providing insights into its pathophysiological processes and paving the way for clinical translational research in this domain.

Keywords: Phosphodiesterase 4B, positron emission tomography, radioligand, depression rat model

Introduction

Phosphodiesterase 4 (PDE4) is a key member of the phosphodiesterase family, responsible for the specific hydrolysis of cyclic adenosine monophosphate (cAMP). By modulating cAMP concentrations, PDE4 triggers downstream phosphorylation cascades, regulating various physiological processes, including macrophage activation, cardiac contraction, vasodilation, learning, memory, and emotional responses [1]. Based on upstream conserved regions (UCR1 and UCR2) between the N-terminal and catalytic regions, PDE4 is categorized into long, short, and ultrashort isoforms. The long isoform contains both UCR1 and UCR2, the short isoform includes only UCR2, and the ultrashort isoform has a truncated UCR2 [2]. UCR1 and UCR2 are involved in PDE4 dimerization; phosphorylation of the PKA site on UCR1 weakens UCR1-UCR2 interaction, enhancing PDE4 activity [3, 4]. The PDE4 inhibitor Rolipram has demonstrated antidepressant efficacy in rodents and humans [5, 6]; however, it also induces adverse effects such as nausea, vomiting, and anxiety [7, 8], likely due to inhibition of the PDE4 subtype responsible for the vomiting reflex [9]. The PDE4 family comprises four subtypes: PDE4A, PDE4B, PDE4C and PDE4D [10]. These subtypes share conserved catalytic domains, C-terminal regions, and N-terminal sequences but exhibit distinct biological distributions and functions. PDE4A is associated with cognition and memory, while PDE4C is predominantly expressed peripherally, with minimal central nervous system presence. PDE4D, primarily localized in the nucleus of the solitary tract, is implicated in the emetic effects of PDE4 inhibitors [9, 11].

This study focuses on the role of PDE4B in emotional regulation and its relationship with depression. Recent studies have increasingly focused on the role of PDE4B in the mechanisms underlying depressive symptoms. Basic experiments using animal models have shown that antidepressant interventions with fluoxetine and tricyclic desipramine reduce PDE4B expression in the hippocampus but leave expression in the cerebral cortex unchanged [12]. Similarly, in SD rats treated with antidepressants, fluctuations in PDE4B expression were observed in the hippocampus and frontal cortex [13]. In chronic unpredictable mild stress (CUMS) mouse models, PDE4B expression increased in the control group but decreased following treatment [14]. However, studies on PDE4B expression in humans remain limited. A post-mortem analysis of brain specimens from patients with depression revealed elevated PDE4B protein levels in the cingulate cortex [15]. Additionally, a comparative study of peripheral blood indexes in patients with depression

https://doi.org/10.62347/AXTL7711

before and after antidepressant treatment found significantly increased PDE4B mRNA levels before treatment, which decreased post-treatment [16]. While these findings suggest a correlation between PDE4B expression and depression, they do not establish a definitive pattern of expression changes. Furthermore, these studies rely exclusively on *in vitro* methods, lacking *in vivo* quantitative research to elucidate PDE4B's specific expression and distribution in the brain during depression. This gap in knowledge hinders a comprehensive understanding of PDE4B's role in depression, limiting its potential as a target for drug development and impeding the formulation of effective treatment strategies.

Positron emission tomography (PET) is a powerful molecular imaging tool that noninvasively detects the distribution and function of biological targets *in vivo* [17-19]. In this study, we utilize a PDE4B-targeted probe to image PDE4B expression in the living brain, addressing the current need of *in vivo* quantitative research on PDE4B. In 2017, Pfizer introduced a PDE4B-targeted PET probe, [^{18}F] PF-06445974 [20]. Subsequently, in 2022, Wakabayashi et al. reported brain imaging studies in monkeys and humans. The tracer effectively quantified PDE4B expression in the human brain, showing promise for clinical applications [21]. The Chronic Unpredictable Mild Stress (CUMS) model stands as one of the preeminent animal models at present. By mimicking adverse stress events in human life, it subjects rats to an environment of unpredictable mild stress over an extended period [22]. This chronic exposure triggers the emergence of depressive-like behaviors and physiological alterations in rats, rendering the model a common choice for investigating the pathogenesis of depression and the mechanisms underlying the action of antidepressant drugs [23]. Our study employs [^{18}F]PF-06445974-PET to quantitatively analyze PDE4B expression in the depression brain. The findings aim to provide a visual foundation for exploring its underlying physiological mechanisms and offering a scientific basis for precise targeted therapies, for drug development for depression.

Materials and methods

Radiochemistry

The synthesis of the cold standard, precursor and radiosynthesis of [^{18}F]2 were accomplished based on published protocols with modifications [21]. The radiosynthesis was conducted using a TRACERlab® FX2 N module. First, a proton beam generated by the Minitracer Qilin 10.0 MeV cyclotron (GE, USA) bombarded > 98% enriched $H_2{}^{18}O$ (TAIYO NIPPON SANSO Corporation, Tokyo, Japan) to produce [^{18}F]fluoride. The [^{18}F]fluoride was trapped using a pre-treated Sep-Pak QMA Plus Light cartridge (Waters cat. no. 186004540) and eluted with a solution of TEAB (2.0 mg) in CH_3CN/H_2O (v/v, 7/3, 1.0 mL) into a 4 mL reaction vial. The eluate was evaporated and dried under nitrogen at 65°C for 5 min, followed by 110°C for 8 min. Next, the precursor (0.5 mg) was dissolved in DMF (0.5 mL) and added to the reaction vial. The reaction was carried out at 120°C for 10 min. The reaction mixture was quenched and diluted with MeCN (1.0 mL) and water (1.5 mL), and subsequently purified using semi-preparative HPLC (OSAKA SODA CAPCELL PAK C18, UG80, 5 μm, 10 × 250 mm) with a mobile phase of CH_3CN/H_2O (v/v, 3/7) at a flow rate of 5 mL/min. The retention time (t_R) of [^{18}F]2 was 26 minutes. Finally, the collected [^{18}F]2 fraction was diluted with 60 mL of sterile water and passed through a Sep-Pak light C18 (Waters cat. no. WAT023501). The cartridge was rinsed with 20 mL of sterile water, and [^{18}F]2 was eluted with ethanol (1 mL). The eluate was diluted with saline (9 mL) to produce a solution of the ^{18}F-labeled radioactive ligand solution. An analytical HPLC system was used to analyze the radiochemical and chemical purity, which consists of an analytical column from OSAKA SODA (CAPCELL PAK C18, UG80, 5 μm, 4.6 × 250 mm) and a UV detector at 254 nm. An aliquot (100 μL) was co-injected with the non-radiolabeled standard to confirm the identify on the analytical HPLC system with a mobile phase of CH_3CN/H_2O (v/v, 55/45) and a flow rate of 1 mL/min.

In vitro stability evaluation

The formulated [^{18}F]2 solution obtained by automated synthesis was placed at room temperature for 0 min, 30 min, 60 min, 90 min, and 120 min. Radiochemical purity at each time point was analyzed using the previously described analytical HPLC system.

Measurement of Log$D_{7.4}$

An aliquot of [^{18}F]2 (*ca.* 15 μCi) was added to a 15 mL centrifugal tube containing 3.65 mL of 1-octanol (3.0 g) and 3.0 mL of 1 × phosphate-buffered saline (PBS; 3.0 g, 0.1 M, pH 7.4). The mixture was vortexed for 3 min and then centrifuged at 3500 rpm for 5 min. An aliquot of PBS and n-octanol (0.6 mL each) was removed, weighted and their radioactivity in each component was measured using a 2480 Wizard automatic gamma counter (Perkin Elmer, USA). All counts were decay- and background-corrected. This procedure was repeated until consistent Log$D_{7.4}$ values were obtained, with six consecutive equilibration performed for each Log$D_{7.4}$ measurement. The Log$D_{7.4}$ value was determined by using the following equation: Log [ratio of radioactivity between the *n*-octanol and PBS solutions] (n = 6).

In vitro autoradiography

The brains of wild-type male Sprague-Dawley rats (7-8 weeks old, 220-250 g) were sectioned into 20 μm slices and subsequently stored at -80°C for subsequent experiments. First, the slices were dried under a stream of cold air and incubated for 20 minutes in a buffer solution (50 mM TRIS-HCl, pH 7.4; Addition of 1 mM $MgCl_2$, 1 mM $CaCl_2$, 2 mM KCl and 120 mM NaCl). For baseline condi-

tions, slices were incubated in the buffer containing [^{18}F]2 (50 μCi in 180 mL of buffer) for 60 minutes. To confirm the saturability of binding sites and conduct homologous competition experiments to estimate the dissociation constant (K_D) of [^{18}F]2, the radioligand solution was supplemented with varying concentrations of unlabeled 2 (0.0457 nM to 0.1 μM). Following incubation, the solution was removed, and the slides were rinsed twice with cold buffer for 2 minutes each, followed by a 10-second immersion in cold water to terminate the incubation. Finally, for quantification, a standard curve was prepared by adding a small amount of a diluted probe stock solution (generally about 2 μL) onto prepared paper. The brain slices and standard curve paper were exposed to an imaging plate (Amersham Typhoon; Cytiva, USA) for 30 minutes. Autoradiograms were generated, and photostimulated luminescence (PSL) values for the whole brain were analyzed using a Bio-Imaging Analyzer System (Multi Gauge Version 2.3, FUJIFILM).

For comparison between depression and normal control, the brain slices were incubated in the buffer containing [^{18}F]2 (50 μCi in 180 mL of buffer) for 60 minutes. Following incubation, the slides were rinsed twice with cold buffer for 2 minutes each, followed by a 10-second immersion in cold water to terminate the incubation. Finally, Autoradiograms were generated and photostimulated luminescence (PSL) values in the cerebral cortex and hippocampus were performed using a Bio-Imaging Analyzer System. Then, the PSL values per unit area were compared.

Radiometabolite analysis

Under isoflurane anesthesia, SD rats were injected with [^{18}F]2 (15-25 MBq) via the tail vein and sacrificed at 20- and 60-minutes post injection (n = 3 per time point). Blood and brain tissues were rapidly collected for analysis. Blood samples were centrifuged at 6,000 rpm at 4°C for 5 minutes to separate plasma. A 0.5 mL aliquot of supernatant was collected in a test tube containing CH_3CN (0.5 mL), vortexed for 30 seconds, and centrifuged at 14,000 rpm for 3 minutes at 4°C for deproteinization and the resulting supernatant was collected for further analysis. Similarly, rat brain samples were homogenized with 1 mL CH_3CN, followed by centrifugation at 14,000 rpm for 3 minutes at 4°C. The resulting supernatant was collected. Supernatants collected from blood and brain samples were mixed with water, respectively. To this mixture, 50 μL of 2 (PF-06445974, 1 mg/mL) was added. The samples were then injected into a semi-preparative high performance liquid chromatography using an OSAKA SODA CAPCELL PAK C18 column (UG80, 5 μm, 10 × 250 mm). The mobile phase consisted of CH_3CN/H_2O (v/v, 55/45) at a flow rate of 4 mL/min. Fractions were collected every 30 seconds over 15 minutes, and radioactivity in each tube was measured using a 2480 Wizard automatic gamma counter (PerkinElmer, USA). Radioactivity counts were corrected for decay, and the radiochromatogram was reconstructed. The percentage of [^{18}F]2 (standard UV peak as a percentage of HPLC) in total radioactivity was calculated as the ratio of the radioactivity in tubes 9-13 to the total radioactivity across all tubes, i.e., [(counts for tube 9-13)/(total tube)] × 100.

PET-CT imaging studies

PET/CT imaging was performed using an IRIS small animal PET/CT imaging system (inviscan SAS, Strasbourg, France). Wild-type SD rats were anesthetized with 2.5-3% (v/v) isoflurane and maintained at 37°C using a heated air circulation system during scans. The radiotracer (15-25 MBq/150-200 μL) was administered via a pre-installed tail vein catheter. Dynamic emission scans in a three-dimensional list mode were conducted for 120 min (20 s × 6 frames, 30 s × 8 frames, 60 s × 4 frames, 120 s × 5 frames, 240 s × 5 frames, 300 s × 16 frames, frames for each rat). For pretreatment studies, 2 (0.1 mg/kg) or Rolipram (1 mg/kg) dissolved in 1 mL of saline containing 5% DMSO and 5% Tween 80 was injected 10 minutes prior to the administration of [^{18}F]2. For displacement ("chase") studies, 2 (0.1 mg/kg) was injected at 60 min via the tail vein catheter following the injection of [^{18}F]2. PET data were reconstructed using a three-dimensional ordered-subset expectation-maximization (3D-OSEM) algorithm with a Monte-Carlo based accurate detector model, and the image voxel is 0.855 × 0.855 × 0.855 mm^3. FDK reconstruction algorithm was used for CT reconstruction, and the image voxel was 0.16 × 0.16 × 0.16 mm^3. PMOD software (version 4.1) was used to generate representative PET images (co-registered with the rat brain MRI template) and analyze the TACs from VOI in the cerebral cortex, striatum, hippocampus, thalamus and cerebellum. The radioactivity was characterized by SUV. SUV = (radioactivity per mL tissue/injected radioactivity) × body weight.

The depressed and control rats were injected with radioactive tracer [^{18}F]2 (15-25 MBq, 150-200 μL) through the tail vein. After 60 min, the rats were anesthetized with isoflurane and then scanned on the machine, followed by 10 minutes static scan and CT scan. Cerebral cortex, hippocampus and cerebellum of interest (ROIs) in the brain were drawn automatically. The standard uptake value (SUV) was calculated for static images. Finally, each regional SUV (mean) was divided by the cerebellum SUV to derive a relative SUV (SUVR) for statistical analysis. This semi-quantitative approach can counteract some of the factors that affect SUVs such as individual differences.

Depression rat brain study

Animals: Male SD rats (180-200 g) used in the study were purchased from Beijing Huafukang Biotechnology Co., LTD. License number: SCXK (Beijing) 2019-0008. The rats were housed in an SPF environment with controlled conditions (temperature: 20-26°C; humidity: 40%-70%)

with ad libitum access to food and water. Rats were acclimatized for seven days prior to the experiments. All animal experiments involved in this study were approved by the Experimental Animal Management and Ethics Committee of Jinan University.

Chronic unpredictable mild stress (CUMS) protocol: Following a one-week acclimation period, control animals remained in a comparable environment. The CUMS procedure in this study was based on previously reported methods with minor modifications [21]. The preparation of the CUMS depression model involved the following steps: A. Flash stimulation for 7 h; B. Wet bedding material 17 h; C. 1 cm away from the rat tail, clip the tail for 1 min; D. Lighting overnight; E. Cage tilt 45°C 7 h; F. Combined cage feeding for 17 h; G. Strange abnormal smell (fresh air) 17 h; H. Strange and abnormal items (plastic sheets, wooden spoons, rags, etc.) 7 h; I. Fasting for 10 h; J. After fasting for 10 h, restrict diet for 2 h; K. No water for 10 h; L. After 10 hours of water prohibition, empty the bottle for 1 hour. The above 12 kinds of stimuli were randomly arranged over a 21-day period, with each stimulus appearing no more than 3 times and not consecutively, to ensure unpredictability.

Behavioral testing

Forced swimming test (FST): The forced swimming test (FST) was conducted following the method established by Porsolt et al. [24]. Rats were placed individually in a vertical plexiglass cylinder (22.5 cm in diameter and 50 cm in height) containing 35 cm of water (temperature 22-25°C). The total recording time was 6 minutes, and the experiment was performed using a single blind design. Immobility time, defined as the duration during which the rat floated with minimal movement or remained in a vertical position with only the nose above the water, was recorded.

Sucrose preference test (SPT): Anhedonia, a core symptom of depression, was assessed using the sucrose preference test (SPT) [25]. Two days prior to the formal experiment, a 10% sucrose solution was prepared, and both a sucrose water bottle and a regular drinking water bottle were placed in the cage. The positions of the bottles were alternated every 2 hours over an 8-hour period. One day prior to the test, rats were deprived of water for 24 hours. For the experiment, both bottles were weighed and positioned in the cage. After 2 hours, the remaining volumes of the sucrose and regular water were measured. The sucrose preference rate (%) was calculated using the formula: sucrose consumption mL/(total water + sucrose consumption mL) × 100%.

Statistical analysis

The data were analyzed using GraphPad Prism 9.5.0 (GraphPad, La Jolla, CA, USA) software and are expressed as mean ± standard deviation (SEM). Statistical differences between the control and depression groups were evaluated using a two-tailed unpaired t-test. If an F-test P < 0.05 is encountered during actual operation, Welch's correction was applied to obtain an adjusted *p*-value. A value of $P < 0.05$ was considered statistically significant (*P < 0.05, **P < 0.01, ***P < 0.001, and ****P < 0.0001).

Results

Radiochemistry and in vitro stability

[^{18}F]2 was prepared using the GE TRACERlab® FX2 N synthesizer as shown in **Figure 1A**. [^{18}F]2 was obtained in 10.1 ± 2.2% non-decay corrected final yield (90 ± 3.6 min total synthesis time) with > 99% radiochemical purity and 2.2 ± 1.3 GBq/μmol (n = 11) molar activity. Notably, [^{18}F]2 demonstrated excellent *in vitro* stability, with no evidence of radiolysis detected in ethanol-containing saline (10%) over a period of 120 minutes (**Figure 1B**).

Measurement of lipophilicity

The lipophilicity of compound 2 was determined using the "shake flask method" [26], yielding a Log$D_{7.4}$ value of 2.41 ± 0.02 (n = 6, **Table 1**). This value indicates that [^{18}F]2 possesses favorable lipophilicity for CNS-targeted PET.

In vitro autoradiography

To determine the binding affinity of [^{18}F]2 in the PDE4B-expressing regions of the rat brain, we performed quantitative autoradiography *in vitro*. Quantitative autoradiography has been performed by incubating 20 μm cryosections with 0.3 nM [^{18}F]2 alone or with different concentrations of unlabeled 2 (0.0457 nM-0.1 μM) (**Figure 2A**). Non-linear regression analysis of the homologous inhibition curve for the percentage of specific binding of [^{18}F]2 in the whole brain (GraphPad Prism 9.5.0; Parameters: Nonlinear Regression-Sigmoidal, 4PL, X is log(concentration) [3]) revealed a K_d value of 2.1 ± 0.9 nM (**Figure 2B**). The autoradiography results demonstrated that [^{18}F]2 exhibits high affinity for PDE4B targets in the brain, consistent with IC_{50} values in the low nanomolar range obtained by scintillation proximity test of human recombinant full-length PDE4B [20]. These findings underscore the high binding affinity and inhibitory potency of [^{18}F]2 for PDE4B, highlighting its potential for *in vivo* brain imaging.

Radiometabolite analysis

To evaluate the metabolic stability of [^{18}F]2 *in vivo*, radioactive metabolites in plasma and brain homogenate of SD rats were assessed. Brain and plasma samples were collected at 20 and 60 minutes post-injection, and analyzed using radioactive high performance liquid chromatography and a gamma counter. As shown in **Figure 3**, [^{18}F]2 has excellent *in vivo* stability in the brain with no detectable ^{18}F-labeled metabolites (unchanged fraction > 98% at both two time points). In plasma, [^{18}F]2 exhibited moderate stability, retaining approximately 40% of the

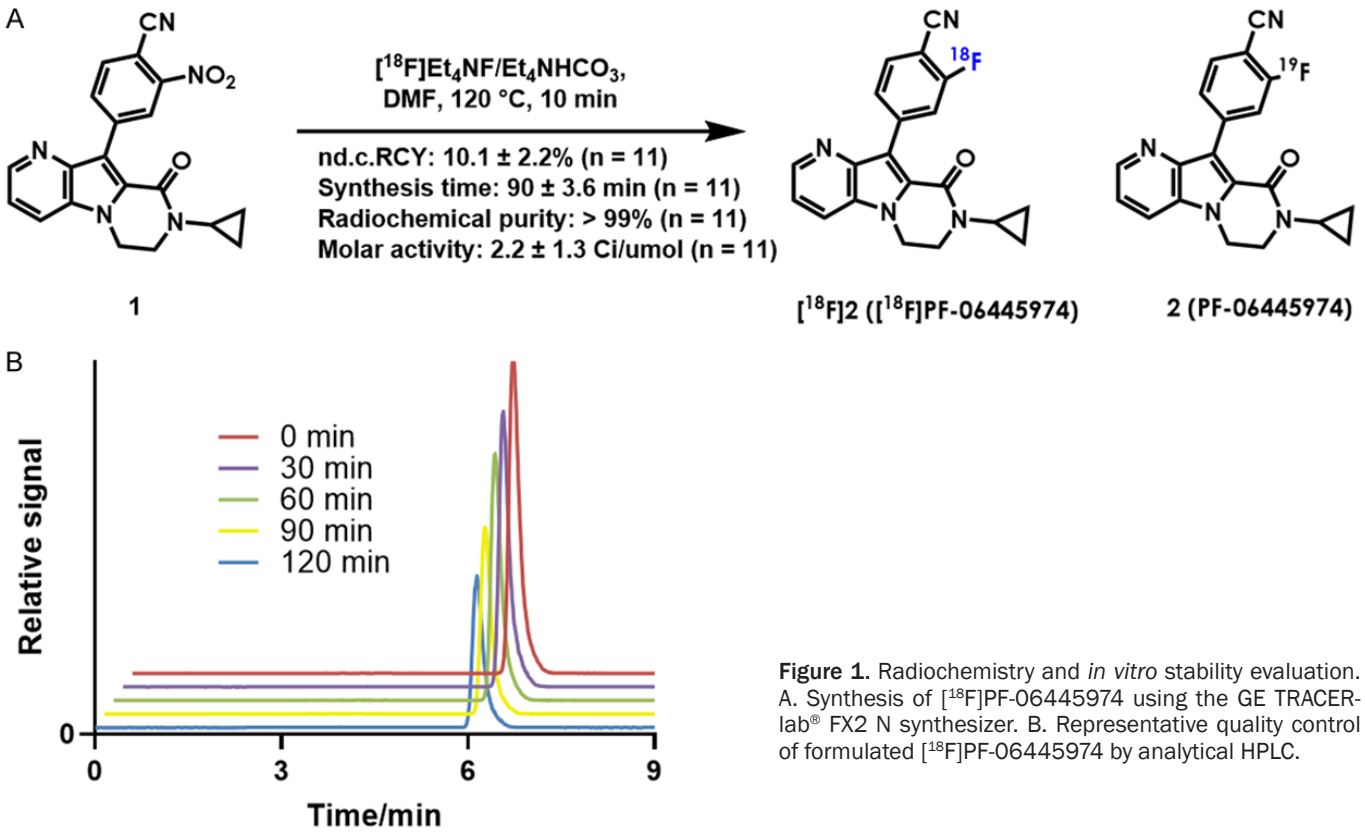

Figure 1. Radiochemistry and *in vitro* stability evaluation. A. Synthesis of [^{18}F]PF-06445974 using the GE TRACERlab® FX2 N synthesizer. B. Representative quality control of formulated [^{18}F]PF-06445974 by analytical HPLC.

Table 1. Assessment of Log*D* values of [^{18}F]2

Tracer:[^{18}F]2				
LogD	2.41			
	CPM	Weight/mg	LogD	average
Oct-1	1352170.69	47.10	2.41	2.41
PBS-1	6772.05	59.84		
Oct-2	1422635.47	49.65	2.38	
PBS-2	7350.41	60.65		
Oct-3	1428598.04	49.68	2.40	
PBS-3	6830.04	59.57		
Oct-4	1231245.16	47.23	2.42	
PBS-4	5897.60	58.97		
Oct-5	1316021.79	50.46	2.41	
PBS-5	6176.74	60.27		
Oct-6	1306309.22	50.10	2.43	
PBS-6	5902.72	60.41		

parent tracer at 20 minutes and 35% at 60 minutes. No radioactive metabolites were detected in the brain, while more polar radioactive metabolites were observed in the plasma. Overall, our results show that radioactive metabolites do not cross the blood-brain barrier, and [^{18}F]2 exhibits reasonable *in vivo* stability for PET imaging studies.

PET imaging studies in normal rat brain

Dynamic PET imaging of [^{18}F]2 was performed in the Sprague-Dawley rat brain for 120 minutes to evaluate the tracer's kinetics and binding specificity. Representative PET images in the brain (horizontal, sagittal and coronal, summed images 0-60 min and 60-120 min) and time-activity curves are shown in **Figure 4**. [^{18}F]2 demonstrated excellent BBB penetration with a maximum standard uptake value (SUV) of 3.3 at 26 minutes post injection in the whole brain. Regional differences in tracer uptake were observed, with the highest uptake in the striatum (SUV_{peak} = 3.4), followed by the thalamus, cortex and hippocampus, while the cerebellum showed the lowest uptake (**Figure 4A**, **4E**). These distribution characteristics of the tracer in normal rat brains were consistent with the distribution of PDE4B enzyme in rodents [20]. As shown in **Figure 4B**, **4C**, **4F** and **4G**, pretreatment with either 2 (0.1 mg/kg, 10 min iv before injection) or rolipram (1 mg/kg, 10 min iv before injection) significantly reduced tracer uptake in selected brain regions, effectively abolishing regional differences. During the pre-blocking experiment with the PDE4 inhibitor Rolipram, the TAC showed an upward trend over time. This is likely attributed to Rolipram having a relatively short half-life (~12 minutes), leading to its rapid clearance and then subsequent reopening of binding sites for [^{18}F]2. As shown in **Figure 4D** and **4H**, the binding of [^{18}F]2 was reversible, as demonstrated by [^{18}F]2 displacement experiment, in which the tracer uptake was reduced by 46 ± 4% (averaged from 5 brain regions) based on the SUV values. Throughout the PET imaging process, no radioactivity was observed in the skull, indicating an absence of radiodefluorination in the body. These collective results confirm the reversible and high specific binding of [^{18}F]2 for PDE4B in rodent brains.

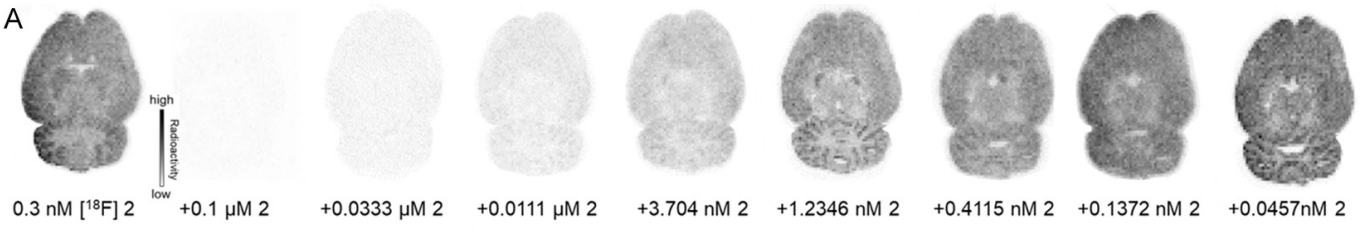

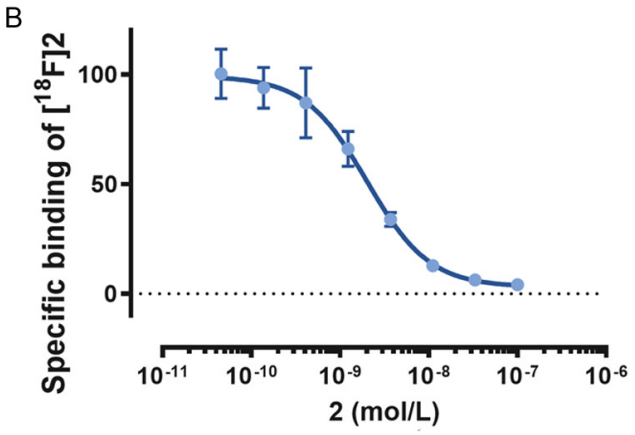

Figure 2. Characterization of the *in vitro* binding sites of [^{18}F]2 in rat brains by homologous competition and determination of the K_D value of the binding of [^{18}F]2 towards rat PDE4B in vitro. A. Representative autoradiograms of 20 μm cryosections of one male SPRD rat incubated with 0.3 nM [^{18}F]2 alone (total binding) or in the presence of different concentrations of 2. B. Competitive binding curves of K_D determination of [^{18}F]2 on PDE4B.

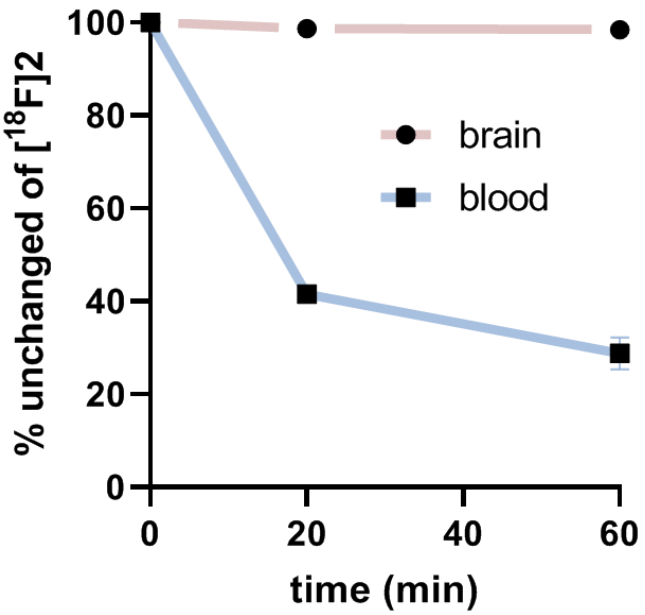

Figure 3. Percentages of unchanged [^{18}F]2 in rat brain tissue and plasma (n = 3) at 20 and 60 min postinjection.

Study on microPET imaging of depression model rat

CUMS induced significant depressive-like behaviors in rats: Following three weeks of CUMS stimulation, behavioral changes in the rats were analyzed by the SPT and FST. An overview of treatment effects on immobility behavior during the FST is presented in **Figure 5A**. The immobility time of rats were significantly increased after CUMS stimulation ($P < 0.0001$). Additionally, the SPT results robustly demonstrated that CUMS led to a subtle yet statistically highly significant reduction in sucrose preference ($P < 0.0001$, **Figure 5B**).

PET imaging studies in rat brains: The [^{18}F]2 PET imaging method was employed to monitor the changes in the expression of PDE4B between rats subjected to CUMS and control group. SUVr values were used to monitor [^{18}F]2 uptake in the whole brain and in specific regions of interest including the cortex and hippocampus (**Figure 5C**, **5D**). It was observed that the accumulation amount of [^{18}F]2 in the hippocampus and cortex of the depression model rats was significantly higher than that in the normal control rats. The results demonstrated that CUMS significantly enhanced the uptake of [^{18}F]2 in both the hippocampus and the cortex regions.

In vitro autoradiography: Autoradiography of [^{18}F]2 targeting the PDE4B receptor revealed a significant increase in radioactivity in the cerebral cortex and hippocampus of depression model rats compared to controls (**Figure 5E**). The grayscale values of each brain region in various brain tissues were quantified, and comparisons were made between each brain region of depression model rats and control rats. The results are expressed in terms of grayscale values per unit area. As shown in **Figure 5F**, in the brains of depression model rats, the grayscale value per unit area in the hippocampal region was higher than that in control rats ($P < 0.05$). Similarly, the grayscale value per unit area in the cortical region was also significantly higher than that in control rats ($P < 0.0001$).

Discussion

The most widely accepted theory in the pathogenesis of depression involves alterations in neurotransmitter levels. For example, changes in serotonin, norepinephrine, and dopamine levels have been associated with the onset of depression. While drugs targeting monoamine neurotransmitter imbalances have shown some clinical effi-

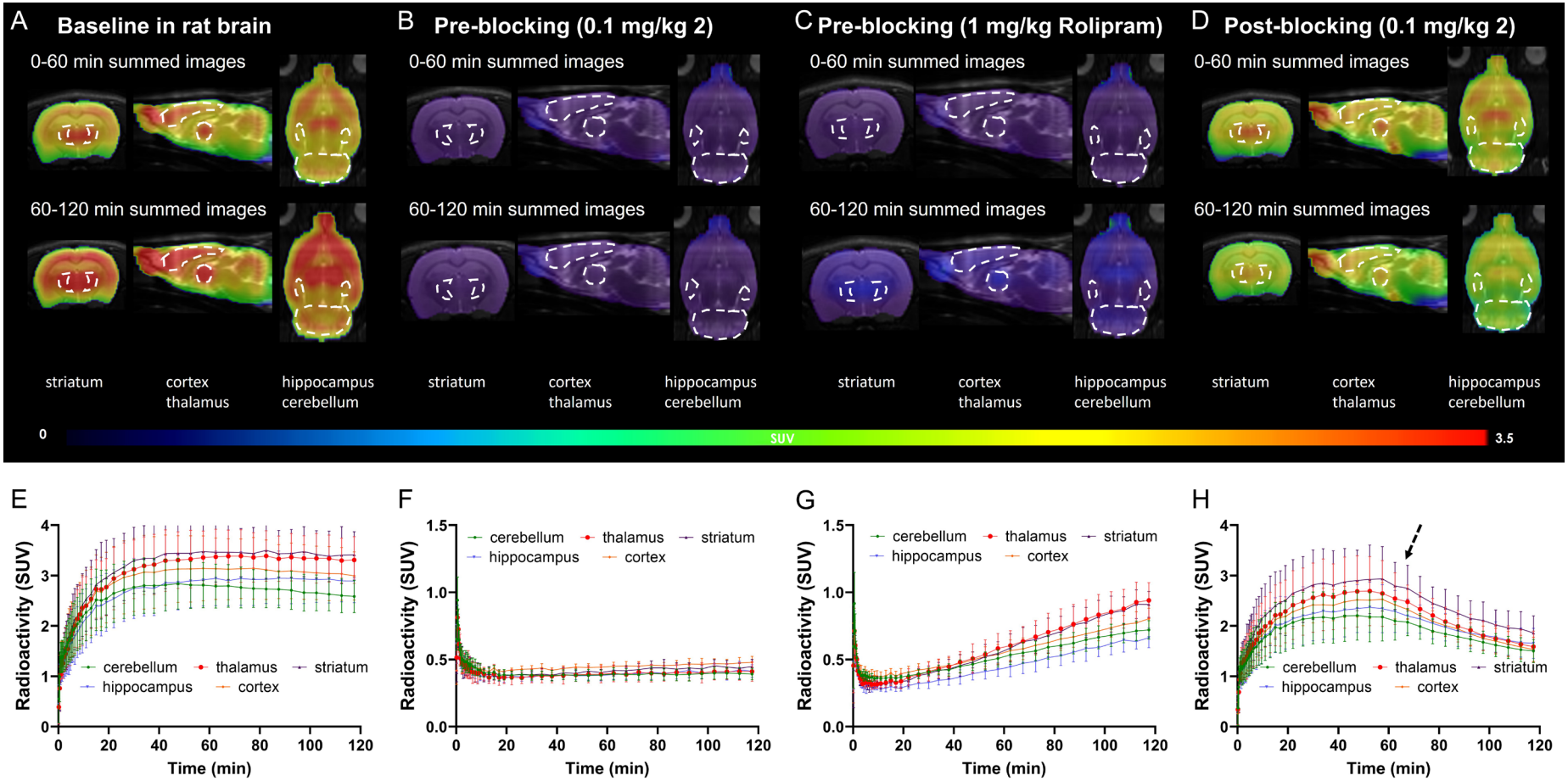

Figure 4. PET studies of [^{18}F]2 in the brain. A, E. Representative PET-MRI images and TACs in various brain regions of interest under baseline conditions; B, F. Representative PET-MRI images and TACs in various brain regions of interest under blocking conditions (pre-injection of 2, i.v); C, G. Representative PET-MRI images and TACs in various brain regions of interest under blocking conditions (pre-injection of Rolipram, i.v); D, H. Representative PET-MRI images and displacement study of [^{18}F]2, with 2 given at 60 min p.i.

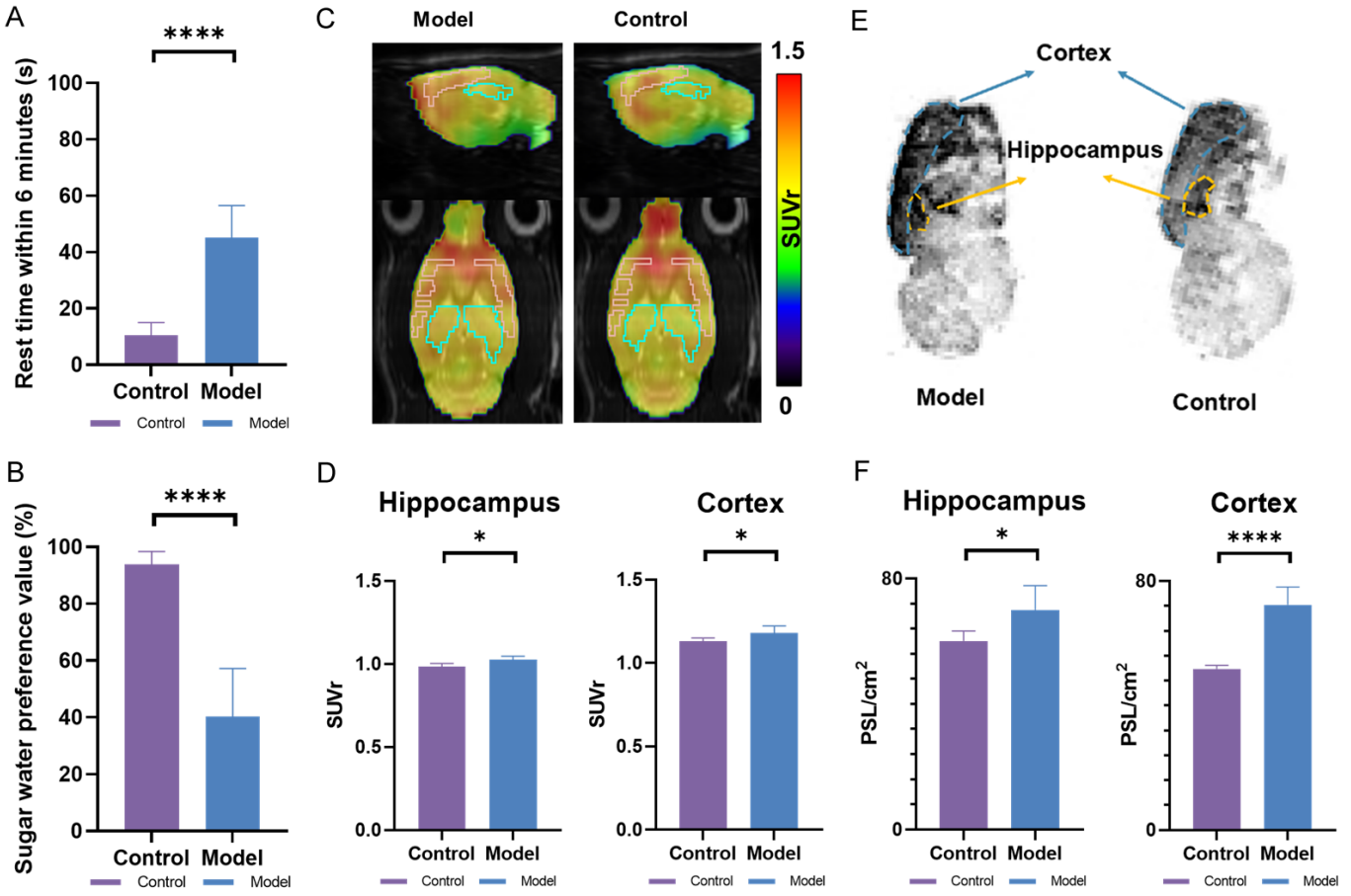

Figure 5. Comparison of behavioral scores and imaging results between model and control groups. A. Forced swimming test after the CUMS procedure (n = 6); B. Percentage rates of sucrose preference test after the CUMS procedure (n = 6); C, D. Representative PET images and SUVr in hippocampus and cortex under baseline condition (n = 6); E, F. Representative ARG images and quantitative analysis of [^{18}F]2 (n = 6). Data were shown as mean ± standard deviations, *P < 0.05, ****P < 0.0001 compared to control group mice.

cacy, their overall treatment efficiency remains suboptimal. Moreover, these medications can impair cognitive function and, in some cases, lead to adverse effects such as suicidal tendencies. Therefore, there is an urgent need to develop novel antidepressants that not only improve mood but also promote cognitive function. Recent advancements in neuroscience have brought increased attention to the neuroinflammation, neurotrophy, and neuroplasticity hypotheses, which have gained extensive recognition. These developments have spurred interest in non-monoaminergic drugs targeting the regulation of these biological processes. One such example is the PDE4 inhibitor, Rolipram, which has demonstrated antidepressant effects in both rodents and humans [5]. Our research focuses on the relationship between PDE4B and depression, utilizing PET imaging to explore *in vivo* distribution and quantitative biological information related to PDE4B in depressive disorders. This study introduces a novel ^{18}F-labeled PDE4B-targeted PET radiotracer, [^{18}F] PF-06445974, and evaluates its potential of imaging PDE4B in the rat brain. [^{18}F]2 was synthesized using the GE TRACERlab® FX2 N automated synthesis module, following a method reported in the literature. [^{18}F]2 demonstrated high radiochemical purity, favorable yield, and specific activity, making it suitable for convenient synthesis and potential clinical application. In addition, [^{18}F]2 exhibited excellent stability, remaining intact for up to 2 hours post formulation. Its Log$D_{7.4}$ lies within the optimal range for BBB penetration. Autoradiographic studies indicated that [^{18}F]2 binds with high affinity and high specificity to PDE4B in the brain. The affinity and inhibitory potency of [^{18}F]2 for PDE4B fall within the low-nanomolar range, supporting its potential as a promising PET imaging agent for *in vivo* studies of PDE4B in the brain.

To evaluate the kinetic profile of [^{18}F]2 in rodents, PET imaging study and radiometabolite analysis experiments were conducted. The results demonstrated that [^{18}F]2 exhibits excellent BBB penetration and reversible, PDE4B-specific binding in rodents. No radioactivity was detected in the skull during the PET imaging process, indicating that [^{18}F]2 does not undergo radioactive radiodefluorination *in vivo*. Radiometabolite analysis confirmed that radioactive metabolites cannot cross the BBB, and [^{18}F]2 exhibits high stability *in vivo*.

The CUMS method, widely recognized as a model for inducing depression through environmental stressors, closely mirrors the pathogenesis of human depression.

This method is particularly suitable for studying the underlying mechanisms of depression and for screening potential therapeutic agents. While previous research has suggested a correlation between PDE4B and the development of depression, changes in PDE4B expression have not been fully elucidated. In this study, the PDE4B-targeted probe [^{18}F]2 was employed to investigate PDE4B expression in the brains of CUMS rats. *In vivo* PET studies demonstrated significantly increased uptake of [^{18}F]2 in the hippocampal and cortical regions of CUMS rats compared to normal control rats. Similarly *in vitro* autoradiography revealed a substantial concentration of radioactivity in the hippocampal and cortical regions of CUMS rats, consistent with the *in vivo* findings. According to the existing studies, immunohistochemistry results show increased PDE4B expression in the hippocampus of mice subjected to the chronic unpredictable mild stress (CUMS) model [14]. Additionally, western blot analyses revealed elevated PDE4B expression in the cortex of individuals with depression [15]. However, it is important to note that the study does not include molecular biology experiments to validate the observed changes in PDE4B expression. Despite this limitation, [^{18}F]2 has proven to be a valuable tool for visualizing dynamic changes in PDE4B expression associated with depressive disorders. This radiotracer enables a deeper understanding of the role of PDE4B in the onset and progression of depression and provides a platform for assessing the efficacy of novel antidepressant therapies.

Conclusion

In this study, we, for the first time to our knowledge, evaluated a rat model of depression using quantitative PET imaging with [^{18}F]PF-06445974. The results demonstrated significant increases in PDE4B expression in the hippocampal and cortical regions of the depression model rats. The consistency between *in vivo* PET imaging and *in vitro* autoradiography further underscores the reliability of these findings. These data highlight the potential of *in vivo* PDE4B-targeted PET imaging as a valuable tool for assessing depression. This approach provides novel insights into the pathophysiological processes underlying depression and holds promise for advancing clinical translational research in this field.

Acknowledgements

We would like to thank the staff at the radiochemistry program at the Department of Nuclear Medicine, the First Affiliated Hospital of Jinan University for their support with cyclotron operation and radioisotope production. This work was supported by the National Natural Science Foundation of China (No. 82300567), Guangzhou Science and Technology Program, China (202206010106), Guangzhou Basic and Applied Basic Research Foundation (202201010536), and the Construction Project of Shanghai Key Laboratory of Molecular Imaging (18DZ2260400).

Disclosure of conflict of interest

None.

Address correspondence to: Steven H Liang, Department of Radiology and Imaging Sciences, Emory University, 1364 Clifton Road, Atlanta, GA 30322, USA. E-mail: steven.liang@emory.edu; Lu Wang, Center of Cyclotron and PET Radiopharmaceuticals, Department of Nuclear Medicine and Key laboratory of Basic and Translational Research on Radiopharmaceuticals, The First Affiliated Hospital of Jinan University, Guangzhou 510630, Guangdong, China. E-mail: l_wang1009@foxmail.com

References

[1] Sun J, Xiao Z, Haider A, Gebhard C, Xu H, Luo HB, Zhang HT, Josephson L, Wang L and Liang SH. Advances in cyclic nucleotide phosphodiesterase-targeted pet imaging and drug discovery. J Med Chem 2021; 64: 7083-7109.

[2] Azevedo MF, Faucz FR, Bimpaki E, Horvath A, Levy I, de Alexandre RB, Ahmad F, Manganiello V and Stratakis CA. Clinical and molecular genetics of the phosphodiesterases (PDEs). Endocr Rev 2014; 35: 195-233.

[3] Richter W and Conti M. Dimerization of the type 4 cAMP-specific phosphodiesterases is mediated by the upstream conserved regions (UCRs). J Biol Chem 2002; 277: 40212-40221.

[4] Beard MB, Olsen AE, Jones RE, Erdogan S, Houslay MD and Bolger GB. UCR1 and UCR2 domains unique to the cAMP-specific phosphodiesterase family form a discrete module via electrostatic interactions. J Biol Chem 2000; 275: 10349-10358.

[5] Wachtel H. Potential antidepressant activity of rolipram and other selective cyclic adenosine 3',5'-monophosphate phosphodiesterase inhibitors. Neuropharmacology 1983; 22: 267-272.

[6] Zeller E, Stief HJ, Pflug B and Sastre-y-Hernández M. Results of a phase II study of the antidepressant effect of rolipram. Pharmacopsychiatry 1984; 17: 188-190.

[7] Heaslip RJ and Evans DY. Emetic, central nervous system, and pulmonary activities of rolipram in the dog. Eur J Pharmacol 1995; 286: 281-290.

[8] Hebenstreit GF, Fellerer K, Fichte K, Fischer G, Geyer N, Meya U, Sastre-y-Hernández M, Schöny W, Schratzer M, Soukop W, Trampitsch E, Varosanec S, Zawada E and Zöchling R. Rolipram in major depressive disorder: results of a double-blind comparative study with imipramine. Pharmacopsychiatry 1989; 22: 156-160.

[9] Richter W, Menniti FS, Zhang HT and Conti M. PDE4 as a target for cognition enhancement. Expert Opin Ther Targets 2013; 17: 1011-1027.

[10] Lugnier C. The complexity and multiplicity of the specific cAMP phosphodiesterase family: PDE4, open new adapted therapeutic approaches. Int J Mol Sci 2022; 23: 10616.
[11] Lamontagne S, Meadows E, Luk P, Normandin D, Muise E, Boulet L, Pon DJ, Robichaud A, Robertson GS, Metters KM and Nantel F. Localization of phosphodiesterase-4 isoforms in the medulla and nodose ganglion of the squirrel monkey. Brain Res 2001; 920: 84-96.
[12] Dlaboga D, Hajjhussein H and O'Donnell JM. Regulation of phosphodiesterase-4 (PDE4) expression in mouse brain by repeated antidepressant treatment: comparison with rolipram. Brain Res 2006; 1096: 104-112.
[13] Takahashi M, Terwilliger R, Lane C, Mezes PS, Conti M and Duman RS. Chronic antidepressant administration increases the expression of cAMP-specific phosphodiesterase 4A and 4B isoforms. J Neurosci 1999; 19: 610-618.
[14] Zhang X, Li X, Li M, Ren J, Yun K, An Y, Lin L and Zhang H. Venlafaxine increases cell proliferation and regulates DISC1, PDE4B and NMDA receptor 2B expression in the hippocampus in chronic mild stress mice. Eur J Pharmacol 2015; 755: 58-65.
[15] Yuan P, Tragon T, Xia M, LeClair CA, Skoumbourdis AP, Zheng W, Thomas CJ, Huang R, Austin CP, Chen G and Guitart X. Phosphodiesterase 4 inhibitors enhance sexual pleasure-seeking activity in rodents. Pharmacol Biochem Behav 2011; 98: 349-355.
[16] Numata S, Iga J, Nakataki M, Tayoshi S, Taniguchi K, Sumitani S, Tomotake M, Tanahashi T, Itakura M, Kamegaya Y, Tatsumi M, Sano A, Asada T, Kunugi H, Ueno S and Ohmori T. Gene expression and association analyses of the phosphodiesterase 4B (PDE4B) gene in major depressive disorder in the Japanese population. Am J Med Genet B Neuropsychiatr Genet 2009; 150B: 527-534.
[17] Rong J, Haider A, Jeppesen TE, Josephson L and Liang SH. Radiochemistry for positron emission tomography. Nat Commun 2023; 14: 3257.
[18] Deng X, Rong J, Wang L, Vasdev N, Zhang L, Josephson L and Liang SH. Chemistry for positron emission tomography: recent advances in ^{11}C-, ^{18}F-, ^{13}N-, and ^{15}O-labeling reactions. Angew Chem Int Ed Engl 2019; 58: 2580-2605.
[19] Krishnan HS, Ma L, Vasdev N and Liang SH. ^{18}F-labeling of sensitive biomolecules for positron emission tomography. Chemistry 2017; 23: 15553-15577.
[20] Zhang L, Chen L, Beck EM, Chappie TA, Coelho RV, Doran SD, Fan KH, Helal CJ, Humphrey JM, Hughes Z, Kuszpit K, Lachapelle EA, Lazzaro JT, Lee C, Mather RJ, Patel NC, Skaddan MB, Sciabola S, Verhoest PR, Young JM, Zasadny K and Villalobos A. The discovery of a novel phosphodiesterase (PDE) 4B-preferring radioligand for positron emission tomography (PET) imaging. J Med Chem 2017; 60: 8538-8551.
[21] Wakabayashi Y, Stenkrona P, Arakawa R, Yan X, Van Buskirk MG, Jenkins MD, Santamaria JAM, Maresca KP, Takano A, Liow JS, Chappie TA, Varrone A, Nag S, Zhang L, Hughes ZA, Schmidt CJ, Doran SD, Mannes A, Zanotti-Fregonara P, Ooms M, Morse CL, Zoghbi SS, Halldin C, Pike VW and Innis RB. First-in-human evaluation of ^{18}F-PF-06445974, a PET radioligand that preferentially labels phosphodiesterase-4B. J Nucl Med 2022; 63: 1919-1924.
[22] Jiang N, Wang H, Huang H, Lv J, Zeng G, Wang Q, Bao Y, Chen Y and Liu X. The antidepressant-like effects of shen yuan in a chronic unpredictable mild stress rat model. Front Psychiatry 2021; 12: 622204.
[23] Becker M, Pinhasov A and Ornoy A. Animal models of depression: what can they teach us about the human disease? Diagnostics (Basel) 2021; 11: 123.
[24] Porsolt RD, Bertin A and Jalfre M. Behavioral despair in mice: a primary screening test for antidepressants. Arch Int Pharmacodyn Ther 1977; 229: 327-336.
[25] Willner P, Towell A, Sampson D, Sophokleous S and Muscat R. Reduction of sucrose preference by chronic unpredictable mild stress, and its restoration by a tricyclic antidepressant. Psychopharmacology (Berl) 1987; 93: 358-364.
[26] Zheng C, Holden D, Zheng MQ, Pracitto R, Wilcox KC, Lindemann M, Felchner Z, Zhang L, Tong J, Fowles K, Finnema SJ, Nabulsi N, Carson RE, Huang Y and Cai Z. A metabolically stable PET tracer for imaging synaptic vesicle protein 2A: synthesis and preclinical characterization of [^{18}F]SDM-16. Eur J Nucl Med Mol Imaging 2022; 49: 1482-1496.